TEXAS TECH UNIVERSITY
Libraries™

ILLUSTRATIVE ANALYSIS OF PROBABILISTIC SEA LEVEL RISE HAZARD

Illustrative Analysis of Probabilistic Sea Level Rise Hazard

MATTHEW A. THOMAS[a]

Department of Civil, Construction, and Environmental Engineering, Marquette University, Milwaukee, Wisconsin

TING LIN[b]

Department of Civil, Environmental, and Construction Engineering, Texas Tech University, Lubbock, Texas

(Manuscript received 2 May 2019, in final form 9 November 2019)

ABSTRACT

Sea level rise results from several contributing physical processes, including ocean thermal expansion and glacier and ice sheet mass loss. Future projections of sea level remain highly uncertain due to several sources of aleatory and epistemic uncertainty. Quantifying different sources of sea level rise involves considering possible pathways of future radiative forcing and integrating models of different sea level rise processes. The probabilistic hazard analysis strategy has been proposed for combining sea level rise prediction models and climate forcing scenarios to examine sea level rise prediction uncertainty and the sources of this uncertainty. In this study we carry out an illustrative probabilistic sea level rise hazard analysis using ensembles of sea level rise predictions and emissions scenarios from the literature. This illustrative analysis allows us to estimate the probability that sea level rise will exceed a specified threshold at a given location and time and highlights how sea level rise uncertainty is sensitive to scenario inputs and sea level rise projection modeling choices. Probabilistic hazard is depicted for Earth using sea level rise hazard maps. We also demonstrate how hazard deaggregation can help us quantify the relative contributions of sea level rise sources, prediction models, and climate forcing scenarios to sea level rise hazard. The ice sheet contribution to sea level rise has a large impact on probabilistic projection of sea level rise due to the disagreements between current ice sheet models related to differences in modeling ice sheet instability.

1. Introduction

Sea level rise occurs due to several physical processes, including thermosteric ocean expansion and glacier and ice sheet mass balance contributions. Prediction models for these sources of sea level rise have associated epistemic modeling uncertainty. Uncertainty regarding future rates of greenhouse gas emissions and the resulting climate forcing also impacts sea level rise. Analyzing future sea level rise involves combining these sources of uncertainty. In this study, we illustrate how sea level rise and climate predictions can be combined using probabilistic sea level rise hazard analysis (PSLRHA) (Lin 2012). This is done using prediction model and climate forcing scenario ensembles.

PSLRHA, inspired by probabilistic seismic hazard analysis (PSHA) (Cornell 1968), is used to find the total probability that sea level rise at a given time will exceed a given threshold by considering projections of sources of sea level rise. Sea level rise hazard maps are created to portray the probability that sea level rise will exceed a given threshold at a given point in time, reflecting current models of sea level rise and associated uncertainty. If such maps were provided at a sufficient resolution, decision-makers could use them to find an appropriate local level of sea level rise consistent with a desired level of probability (e.g., a 95% probability that sea level rise would not exceed this level). Hazard deaggregation (Lin and Baker 2011; Lin et al. 2013) is used to find conditional probabilities of different sources of sea level rise for a given hazard threshold, helping highlight the sources with the greatest influence on probabilistic sea level rise estimates at different hazard levels.

Process-based models such as the general circulation models (GCMs) of the climate system are considered effective for simulating thermosteric sea level rise and

[a] ORCID: 0000-0001-8721-9643.
[b] ORCID: 0000-0003-2650-8040.

Corresponding author: Matthew A. Thomas, matthewaaronthomas9@gmail.com

DOI: 10.1175/JCLI-D-19-0320.1

dynamic sea level changes: regional sea level variations associated with density and pressure changes (Taylor et al. 2012; Landerer et al. 2013; DeConto and Pollard 2016). Process-based ice sheet models (ISMs) have been developed to simulate ice sheet evolution, including mass balance changes (Fyke et al. 2011; Winkelmann et al. 2012; Nowicki et al. 2013a,b). Glacier melt contribution can be simulated using semiempirical energy- and flux-based mass balance models (Radić et al. 2013). Mass balance change, such as results from glacier and ice sheet evolution, creates regional variations in sea level rise related to the locations of mass change. Such regional sea level change can be estimated using the sea level equation (Peltier 2004). Sea level rise prediction modeling uncertainty is often estimated using prediction model ensembles (Mengel et al. 2016; Wong et al. 2017). Climate forcing uncertainty generally is considered in the literature using a set of climate forcing pathways that depict different future socioeconomic trends (Nakicenovic et al. 2000; Ebi et al. 2013; IPCC 2013; van Vuuren and Carter 2013; Nauels et al. 2017). Scenarios such as the representative concentration pathways (RCPs) (Moss et al. 2010) span the range of heavy mitigation of CO_2 emissions to business-as-usual emissions rate growth, but do not consider the probabilities of individual scenarios.

This study demonstrates how sea level rise uncertainty can be modeled using the concept of probabilistic hazard analysis (Cornell 1968; Lin 2012). Our goal is not to provide a comprehensive analysis of sea level rise uncertainty, but to illustrate the connections between sea level rise hazard, the sources of sea level rise, and choices of sea level rise models. Probabilistic hazard analysis is carried out in the study using ensembles of RCPs, GCMs, glacier models, and ISMs. The total probability theorem is used to aggregate sources of sea level rise. Where direct simulation data are not available, sources of sea level rise are estimated using emulation methods from the literature. To estimate the probability distribution of future sea level rise, we randomly sample combinations of forcing scenarios and sea level rise prediction models and consider emulation uncertainty for glacier and ice sheet projections. Bayes's rule is used to deaggregate the contributions of sea level rise sources and prediction models; in other words, to find the conditional probabilities of such model or sources given sea level rise exceeds a certain level (Lin and Baker 2011; Lin et al. 2013). Section 2 describes the methods of probabilistic sea level rise hazard analysis. Sources of sea level rise are emulated for the sampling process using different methods described in section 3. Sea level rise hazard maps and deaggregations are discussed in section 4, helping us consider the relative importance of different sea level rise prediction models and climate forcing scenarios. Results and conclusions are summarized in section 5.

2. Probabilistic sea level rise hazard analysis

a. *Aggregation and deaggregation of probabilistic sea level rise hazard*

In this study, sea level rise uncertainty is modeled using projections of different sources of sea level rise and their associated uncertainties (Mengel et al. 2016; Wong et al. 2017). The largest sources of sea level rise, driven by climate changes, are sea level rise due to thermal expansion and sea level rise resulting from glacier and ice sheet mass losses. Multiple prediction models exist for each source, reflecting modeling uncertainty. Modeling uncertainty can be estimated by treating simulations as samples from a probability distribution of possible sea level rise scenarios. Climate forcing uncertainty can be modeled in a similar way using the RCPs or other forcing scenarios.

In probabilistic hazard analysis, the probability $P(S > h)$ that sea level S exceeds a given hazard threshold h accounts for contributions from thermosteric and dynamic sea level rise T, glacier sea level rise G, and ice sheet sea level rise I. For the purposes of this illustrative study, the impact of land water storage is neglected due to the complexity of including this effect and the relatively small impact on global sea level. As depicted in Eq. (1), total sea level rise in this study is modeled as the simple sum of patterns of thermosteric, dynamic, glacier, and ice sheet sea level change:

$$S = T + G + I. \tag{1}$$

$P(S > h)$ is calculated using the total probability theorem, which integrates conditional sea level rise probability distributions associated with projections of the physical sea level rise processes $P(S > h|T, G, I)$ over probability distributions for thermosteric sea level rise $f(T|\Pi_j, \Upsilon_k)$, glacier sea level rise $f(G|\Pi_j, \Upsilon_k, \Gamma_l)$, and ice sheet sea level rise $f(I|\Pi_j, \Upsilon_k, \Phi_m)$. Sea level rise predictions are dependent on choice of RCP Π_j, GCM Υ_k, glacier model Γ_l, and ISM Φ_m. The probabilistic hazard analysis framework could include RCP probabilities $P(\Pi_j)$, GCM probabilities $P(\Upsilon_k)$, glacier model probabilities $P(\Gamma_l)$, and ISM probabilities $P(\Phi_m)$. For the purposes of this illustrative study, we assume that all models and scenarios are equally likely. Equation (2) depicts the application of the total probability theorem.

$$P(S>h)=\sum_{j=1}^{J}\sum_{k=1}^{K}\sum_{l=1}^{L}\sum_{m=1}^{M}\int_T\int_G\int_I P(S>h|T,G,I)f(T|\Pi_j,\Upsilon_k)f(G|\Pi_j,\Gamma_l)f(I|\Pi_j,\Phi_m)P(\Pi_j)P(\Upsilon_k)P(\Gamma_l)P(\Phi_m)dI\,dG\,dT \tag{2}$$

Thermosteric, glacier, and ice sheet sea level rise projections depend on RCP and GCM. Sea level rise model projections are assumed to be independent in this formulation. In reality, feedbacks should exist between such projections, but the simplifying assumption is necessary for the illustrative analysis due to the difficulty and computational cost of pairing atmospheric, ocean, ice sheet, and glacier models (Vizcaino et al. 2015).

Probabilistic sea level rise hazard analysis allows us to examine the impacts of different forcing scenarios as well as sea level rise contribution projections though hazard deaggregation (Cornell 1968; Lin 2012), which finds the conditional probabilities of different forcing scenarios $P(\Pi_j|S>h)$, GCMs $P(\Upsilon_k|S>h)$, glacier models $P(\Gamma_l|S>h)$, or ISMs $P(\Phi_m|S>h)$ given exceedance of a sea level rise threshold,

$$P(\Pi_j|S>h)=\frac{1}{P(S>h)}\sum_{k=1}^{K}\sum_{l=1}^{L}\sum_{m=1}^{M}\int_T\int_G\int_I P(S>h|T,G,I)f(T|\Pi_j,\Upsilon_k)f(G|\Pi_j,\Gamma_l)f(I|\Pi_j,\Phi_m)P(\Pi_j)P(\Upsilon_k)P(\Gamma_l)P(\Phi_m)dI\,dG\,dT, \tag{3}$$

$$P(\Upsilon_k|S>h)=\frac{1}{P(S>h)}\sum_{j=1}^{J}\sum_{l=1}^{L}\sum_{m=1}^{M}\int_T\int_G\int_I P(S>h|T,G,I)f(T|\Pi_j,\Upsilon_k)f(G|\Pi_j,\Gamma_l)f(I|\Pi_j,\Phi_m)P(\Pi_j)P(\Upsilon_k)P(\Gamma_l)P(\Phi_m)dI\,dG\,dT. \tag{4}$$

Such analysis helps us describe the extent to which various aspects of the sea level rise process are related to exceeding different sea level rise values. Equations (3) and (4) depict hazard deaggregation for RCPs and GCMs. Conditional probabilities can be calculated in the same manner for glacier and ice sheet prediction models. Hazard deaggregation can also be performed to find conditional probability distributions of thermosteric $f(T|S>h)$, glacier $f(G|S>h)$, and ice sheet $f(I|S>h)$ sea level rise. Equation (5) depicts the deaggregation for the probability distribution of thermosteric sea level rise. Distributions for glacier and ice sheet sea level rise can be calculated in the same way.

$$f(T|S>h)=\frac{1}{P(S>h)}\sum_{j=1}^{J}\sum_{k=1}^{K}\sum_{l=1}^{L}\sum_{m=1}^{M}\int_G\int_I P(S>h|T,G,I)f(T|\Pi_j,\Upsilon_k)f(G|\Pi_j,\Gamma_l)f(I|\Pi_j,\Phi_m)P(\Pi_j)P(\Upsilon_k)P(\Gamma_l)P(\Phi_m)dI\,dG \tag{5}$$

Deaggregation quantifies the relative contributions of sea level rise sources, prediction models, and climate forcing scenarios to sea level rise hazard. This allows us to consider how sensitive exceeding sea level rise hazard thresholds is to individual sea level rise sources, models, and scenarios. In this illustrative study, deaggregation is performed only for global mean sea level rise projections. Deaggregation of local sea level rise projections is also possible and could be useful for local decision-making purposes given a more comprehensive probabilistic hazard analysis of sufficiently fine resolution.

b. *Sea level rise prediction sampling*

In this study, sea level rise sources are aggregated using a sampling process that iteratively collects a large sample of joint projections of climate forcing and each source of sea level rise given a pool of forcing scenarios and models. Figure 1 depicts the process for selecting

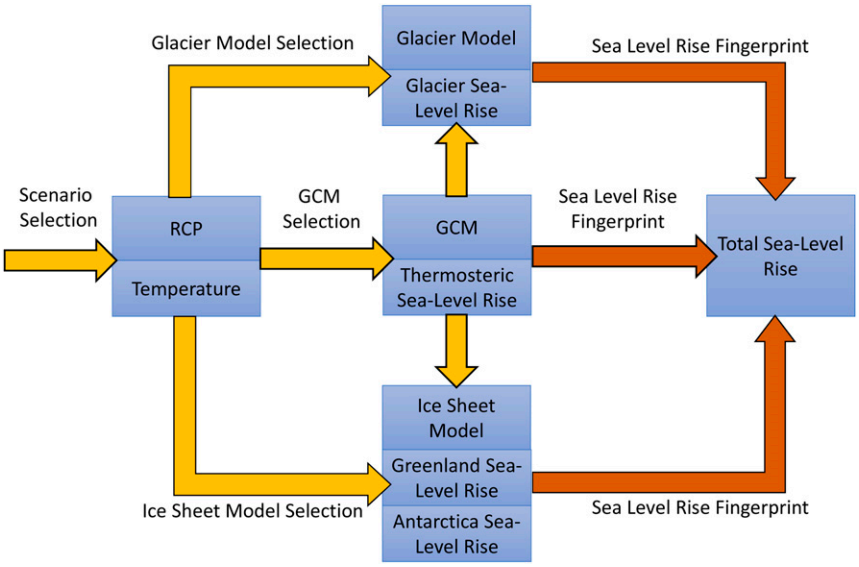

FIG. 1. Flowchart for sampling climate forcing scenarios and sea level rise prediction models for probabilistic sea level rise hazard analysis.

sets of prediction models and forcing scenarios. The sampling process involves several steps:

1) An RCP is selected at random.
2) One of four GCMs is selected at random and corresponding global mean temperature and thermosteric and dynamic sea level rise projections are noted.
3) One of four glacier models are selected at random, and global mean glacier sea level rise for the chosen model and temperature change projection are combined with a randomly sampled pattern of regional glacier sea level rise, estimated from satellite gravimetry data and a sea level equation solver, to produce a glacier sea level rise projection.
4) One of four ISMs are selected, a response-function-based emulation method, which uses a random sample of basal melt sensitivity from a uniform distribution and global mean temperature change, is used to find mass balance change for Greenland and Antarctic ice sheet basins. Mass balance is converted into an ice sheet sea level rise fingerprint using a sea level equation solver.
5) Thermosteric and dynamic sea level rise is combined with glacier and ice sheet sea level rise to produce a sample of overall sea level rise.

A sample size of 10 000 was used in this illustrative study. Iteratively larger sample sizes were tested for the analysis, and it was found that hazard analysis and deaggregation results were not noticeably different between analyses using 5000 and 10 000 samples. A larger sample size could be required for future analyses with larger ensembles of RCPs and sea level rise prediction models or different modeling of stochastic components. We keep track of the RCP, GCM, glacier model, and ISM selected for each sample. In this study, all prediction models and RCPs are assumed to be equally likely.

When a prediction model is selected, specific methods are used to estimate the sea level rise fingerprint associated with that model. GCM thermosteric and dynamic sea level predictions are available directly from model RCP projections. Global mean temperature change time series projections are also taken from these experiments. Glacier and ice sheet mass balance changes are emulated as functions of global mean temperature change using methods from the literature (Slangen and van de Wal 2011; Marzeion et al. 2012; Giesen and Oerlemans 2012; Radić et al. 2013; Levermann et al. 2014). Mass balance changes are converted into sea level rise fingerprints using the sea level equation (Peltier 2004; Adhikari et al. 2016).

3. Modeling and emulating sources of sea level rise

a. Thermosteric and dynamic sea level projection

In the literature, climate forcing scenarios like the RCPs depict a range of possible climate forcing, including mitigation (RCP2.6), business-as-usual (RCP8.5), and moderate (RCP4.5, 6.0) emissions rate growth scenarios for 2006–2100. The phase 5 of the Coupled Model Intercomparison Project (CMIP5) collects GCM climate simulation experiments, including sea level rise projections, for the RCPs (Taylor et al. 2012).

TABLE 1. GCM ensemble members of phase 5 of the Coupled Model Intercomparison Project submodel choices.

GCM name	Modeling group	Ocean submodel	Atmosphere submodel	Land surface submodel
HadGEM2-ES	MOHC	HadGEM2	HadGEM2	HadGEM2
MIROC-ESM	MIROC	MIROC-AGCM	COCO3.4	MATSIRO
MRI-CGCM3	MRI	MRI-AGCM3.3	MRI.COM3	HAL
NorESM1–1-m	NCC	CAM4-Oslo	NorESM-Ocean	CLM4

GCM predictions of thermosteric and dynamic sea level change are available for each RCP and GCM combination considered in this study. A single sea level rise simulation is used for each combination to illustrate how model and scenario ensembles can be built. Multiple simulations for specific experiments are also not available for all GCMs from the CMIP5 datasets. As depicted in Table 1, GCM prediction differences reflect choices in constructing various submodels, such as those of the atmosphere and ocean. An ensemble of GCM projections can help reflect thermosteric and dynamic sea level rise modeling uncertainty.

b. *Glacier model and sea level rise modeling and emulation*

The Intergovernmental Panel on Climate Change (IPCC) Fifth Assessment Report (AR5) (IPCC 2013) identified four glacier models whose projections of glacier mass balance change could be emulated. Table 2 characterizes the relationship between global mean temperature and global mean sea level rise due to glacier melt identified for these models by AR5. The IPCC also estimated the Pearson correlation coefficient ρ for each glacier model between yearly averaged global mean temperature and estimated glacier sea level rise contribution (IPCC 2013).

Glacier global mean sea level rise $G(t)$ at year t is estimated for each sample as a function of temperature above 2006 levels $\Delta\tau(t)$ and the sampled glacier model response parameter γ as described by Eq. (6).

$$G(t) = \sum_{t} \Delta\tau(t)\gamma\, dt. \tag{6}$$

Global mean glacier sea level rise is converted into a pattern of regional glacier sea level change fingerprint by sampling from a selection of fingerprints estimated for glacier mass balance changes measured by the Gravity and Recovery Climate Experiment (Swenson 2012). Monthly measurements of mass balance change for 2006–16 were converted to sea level fingerprints using the sea level equation solver of Adhikari et al. (2016) and then normalized to reflect the pattern of sea level change expected for 1 mm of global mean sea level rise. One normalized glacier pattern is selected for each sample and scaled up to the global mean glacier sea level rise.

c. *Ice sheet and sea level rise emulation*

Physics-based ISMs disagree about the magnitude of future ice sheet contribution to sea level rise. Computationally, these ISMs function like GCMs, using finite-element or finite-difference models to synthesize physics submodels (Nowicki et al. 2013a,b). The computational complexity and relative newness of ISMs makes it difficult to use direct ice sheet simulations in analyses of total sea level rise. In this study, we use a method suggested by Levermann et al. (2014) to emulate ISM projections for different global mean temperature change projections.

This emulation method divides ice sheet mass balance change between an atmospheric response related to global mean atmospheric temperature change and an ocean response related to Arctic ocean temperature change. Mass balance is estimated in this method for seven Greenland ice sheet basins and eight Antarctic ice sheet basins. Change in mass balance at time t due to the time series of global mean atmospheric temperature $\Delta\tau(t_0)$ is modeled at each basin using the response function depicted by Eq. (7).

$$I_a(t) = \int_0^t R_a(t - t_0)\Delta\tau(t_0)\, dt \tag{7}$$

Atmospheric response functions for each ISM are estimated using results from the Sea-Level Response to Ice Sheet Evolution (SeaRISE) project, which collected ISM responses to a variety of atmospheric warming, basal sliding, and ice shelf melting forcing experiments

TABLE 2. Glacier model characteristic responses to global mean temperature and relative reliabilities as estimated by AR5.

Global glacier model	Global mean sea level response (mm $^{\circ}C^{-1}$ yr^{-1})	ρ
Giesen and Oerlemans (2012)	3.02	0.733
Marzeion et al. (2012)	4.96	0.685
Radić et al. (2013)	5.45	0.676
Slangen and van de Wal (2011)	3.44	0.742

TABLE 3. ISM characteristic atmosphere and ocean warming responses estimated for the SeaRISE experiments for Greenland basins.

Basin	100-yr forcing response	AIF	ISSM	SICOPOLIS	UMISM
N basin (82°N, 48°W)	Atmosphere R_a (100) (mm SLE °C^{-1})	−1.11	−0.29	−0.63	−0.51
	Ocean R_o (100) [mm SLE (m yr^{-1})$^{-1}$]	−0.13	−0.01	−0.01	−0.50
NE basin (78°N, 25°W)	Atmosphere R_a (100) (mm SLE °C^{-1})	−0.77	−0.08	−0.36	0.11
	Ocean R_o (100) [mm SLE (m yr^{-1})$^{-1}$]	−0.10	−0.01	−0.04	−0.50
CE basin (70°N, 25°W)	Atmosphere R_a (100) (mm SLE °C^{-1})	0.06	0.08	0.00	0.05
	Ocean R_o (100) [mm SLE (m yr^{-1})$^{-1}$]	0.00	−0.01	0.00	−0.21
SE basin (65°N, 30°W)	Atmosphere R_a (100) (mm SLE °C^{-1})	0.12	0.08	0.00	−0.08
	Ocean R_o (100) [mm SLE (m yr^{-1})$^{-1}$]	−0.01	−0.01	0.00	−0.21
SW basin (65°N, 50°W)	Atmosphere R_a (100) (mm SLE °C^{-1})	−1.32	−0.14	−0.17	−0.59
	Ocean R_o (100) [mm SLE (m yr^{-1})$^{-1}$]	0.00	0.00	0.00	−0.03
CW basin (71°N, 55°W)	Atmosphere R_a (100) (mm SLE °C^{-1})	−0.38	−0.33	−0.39	−0.33
	Ocean R_o (100) [mm SLE (m yr^{-1})$^{-1}$]	0.00	0.00	0.00	−0.38
NW basin (75°N, 60°W)	Atmosphere R_a (100) (mm SLE °C^{-1})	−0.32	−0.09	−0.21	−0.46
	Ocean R_o (100) [mm SLE (m yr^{-1})$^{-1}$]	0.00	0.00	−0.05	−0.31

(Nowicki et al. 2013a,b). In this study, global mean temperature is estimated from the RCP and GCM selected for any given sample. Estimating the ocean contribution to ice sheet mass balance involves converting global mean temperature change to an estimated Arctic ocean temperature. This is done as described by using an estimated scaling coefficient for the ISM used and global mean temperature as described by Eq. (8).

$$\Delta\tau_0(t) = \alpha\Delta\tau(t - t_0) \tag{8}$$

Ocean temperature then is converted to basal melting for the ice sheet basin as a function of basal melt sensitivity as described by Eq. (9):

$$\Delta b = \beta\Delta\tau_0, \tag{9}$$

where β is selected randomly from a uniform observation-based interval between 9 and 16 m yr^{-1} K^{-1} (Levermann et al. 2014). Mass balance change for the basal melting is estimated using another response function estimated from the SeaRISE experiment as depicted by Eq. (10).

$$I_o(t) = \int_0^t R_o(t - t_0)\Delta b(t_0)\, dt. \tag{10}$$

Tables 3 and 4 describe estimated ice sheet responses for Greenland and Antarctic basins and 4 ISM that participated in the SeaRISE project. The $R_a(100)$ and $R_o(100)$ terms for atmospheric and oceanic responses, respectively, reflect values estimated for $t - t_0 = 100$ years via the SeaRISE project (Nowicki et al. 2013a,b). Values are given in terms of sea level equivalent (SLE): the change in global average sea level that would occur if a given amount of water or ice were added to or removed from the oceans.

d. *Sea level rise projection fingerprints*

We can compare the sea level rise fingerprints of different future sea level rise projections as estimated using

TABLE 4. ISM characteristic atmosphere and ocean warming responses estimated for the SeaRISE experiment for Antarctic basins.

Basin	100-yr forcing response	AIF	ISSM	SICOPOLIS	UMISM
QMD (75°S, 40°E)	Atmosphere R_a (100) (mm SLE °C^{-1})	0.17	0.20	−0.08	−0.28
	Ocean R_o (100) [mm SLE (m yr^{-1})$^{-1}$]	−0.25	0.00	−0.20	−1.00
AMR (75°S, 70°E)	Atmosphere R_a (100) (mm SLE °C^{-1})	0.10	0.11	−0.02	0.02
	Ocean R_o (100) [mm SLE (m yr^{-1})$^{-1}$]	−0.15	0.00	−0.15	−1.05
WLK (72°S, 110°E)	Atmosphere R_a (100) (mm SLE °C^{-1})	0.35	0.35	0.53	−0.32
	Ocean R_o (100) [mm SLE (m yr^{-1})$^{-1}$]	−0.03	0.00	−0.03	−1.00
VCT (73°S, 150°E)	Atmosphere R_a (100) (mm SLE °C^{-1})	0.00	0.00	−0.17	0.08
	Ocean R_o (100) [mm SLE (m yr^{-1})$^{-1}$]	0.00	0.00	0.00	−0.65
ROS (82°S, 180°)	Atmosphere R_a (100) (mm SLE °C^{-1})	0.22	0.28	−0.08	−0.10
	Ocean R_o (100) [mm SLE (m yr^{-1})$^{-1}$]	−1.10	0.00	−0.20	−0.40
AMD (73°S, 100°W)	Atmosphere R_a (100) (mm SLE °C^{-1})	0.00	0.00	−0.50	−0.25
	Ocean R_o (100) [mm SLE (m yr^{-1})$^{-1}$]	−0.05	0.00	−0.60	−0.55
PEN (70°S, 70°W)	Atmosphere R_a (100) (mm SLE °C^{-1})	0.10	0.13	−0.33	−0.68
	Ocean R_o (100) [mm SLE (m yr^{-1})$^{-1}$]	−0.03	0.00	−0.20	−0.65
WDL (78°S, 45°W)	Atmosphere R_a (100) (mm SLE °C^{-1})	0.25	0.25	−0.27	0.20
	Ocean R_o (100) [mm SLE (m yr^{-1})$^{-1}$]	−1.25	0.00	−0.55	−0.75

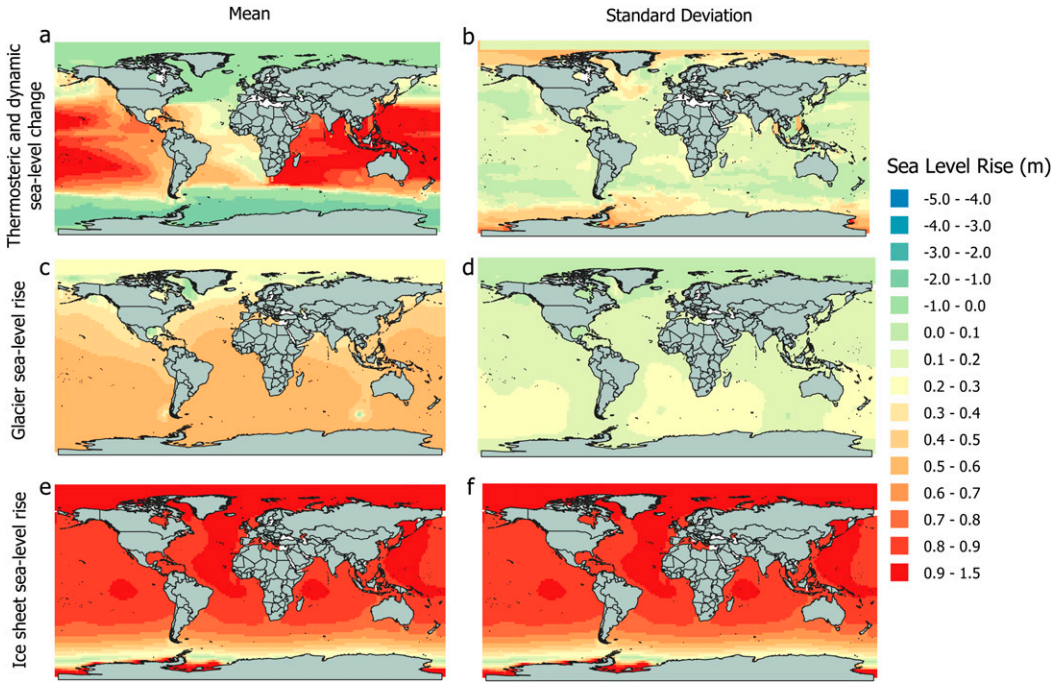

FIG. 2. (a),(b) Mean and standard deviation respectively of GCM and RCP ensemble projections of thermosteric and dynamic sea level change for 2006–2100; (c),(d) mean and standard deviation respectively of glacier model and RCP ensemble projections of glacier sea level rise for 2006–2100; and (e),(f) mean and standard deviation respectively of ISM and RCP ensemble projections of ice sheet sea level rise for 2006–2100.

the prediction model and forcing scenario sampling process. Figure 2 compares sample mean and standard deviation for all sources of sea level rise for 2100 while sampling from all RCPs and prediction models. Given the use of four-member ensembles, the mean and standard deviation do not completely describe the probability distribution, but still give us an idea of regional variations in sea level rise contributions and associated uncertainties. As depicted in Figs. 2a and 2b, variations between GCM sea level rise estimates are relatively small compared to ensemble mean projections. GCMs agree that dynamic sea levels will likely rise at middle latitudes and will likely fall near Antarctica. Ensemble analysis also helps us identify regions of disagreement, such as are apparent at the most northern and southern latitudes. Glacier melt tends to create relatively small sea level impact at more northern latitudes and higher, evenly distributed sea level rise at lower latitudes due to the concentration of glacier mass in the north. Glacier contribution uncertainty is concentrated near the locations of the largest glaciers and at the lowest latitudes, where glacier sea level rise is highest.

Mean and standard deviation of ice sheet sea level rise are much larger than those for thermosteric and dynamic sea level rise and for glacier sea level rise. This reflects the influence of the University of Maine Ice Sheet Model (UMISM), which projects an especially large ice sheet mass balance response to rising temperatures. Mass loss from Greenland causes sea level decreases at northern latitudes and sea level rise at southern latitudes, while mass loss from Antarctica causes the opposite. As depicted in Figs. 2 and 3, regional sea level decreases are much more notable in the south than in the north as sea level rise associated with Antarctica is much larger than that for Greenland.

4. Probabilistic sea level rise hazard mapping and source deaggregation

a. Mapping sea level rise hazard

Sea level rise hazard maps are produced using the results of the sampling process and the total probability theorem. Figure 3 depicts the probabilities that sea level rise will exceed 0.5, 1, 2, 3, and 4 m during the 2006–2100 period. As GCMs have different resolutions based on finite-element resolution choices and glacier data have yet another resolution, all mapped data are found by interpolating individual sea level rise projections onto a $2° \times 2°$ global grid. The probabilities of exceeding a given sea level rise threshold at any grid point are impacted by the regional patterns of sea level rise caused

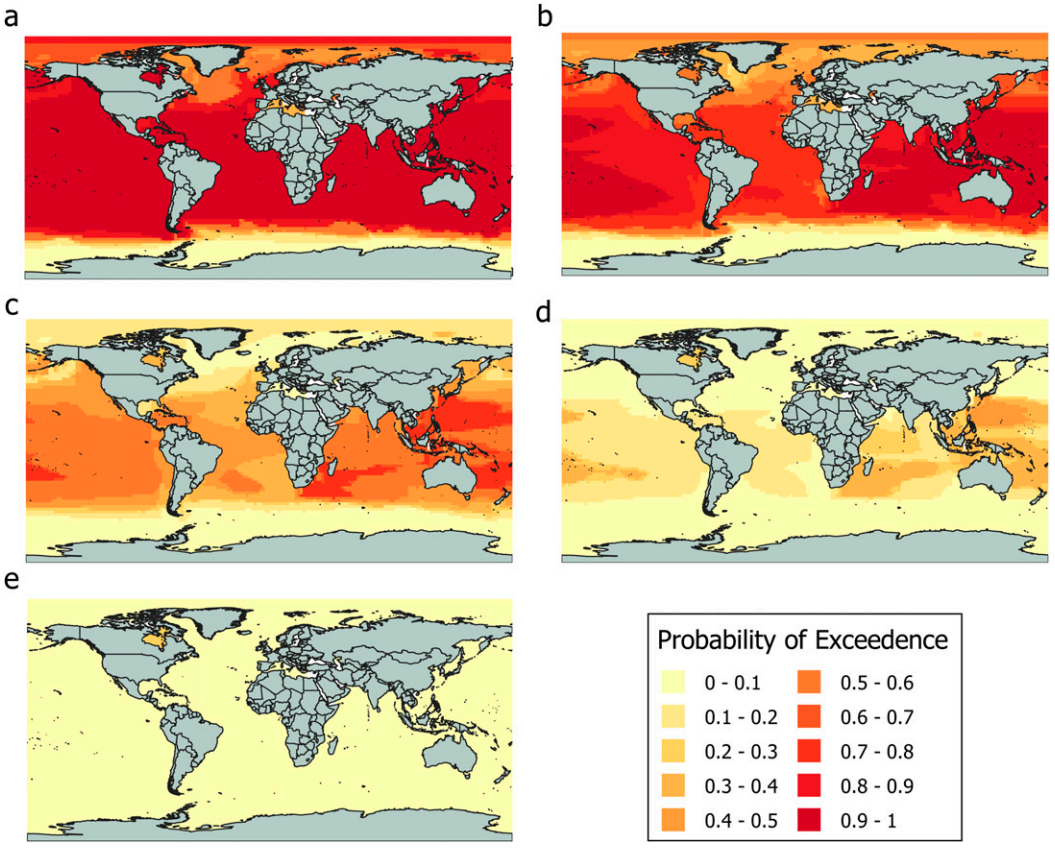

FIG. 3. Probabilities of joint 2006–2100 thermosteric, dynamic, glacier, and ice sheet sea level rise exceeding (a) 0.5, (b) 1, (c) 2, (d) 3, and (e) 4 m.

by dynamic sea level change and ice sheet and glacier mass balance change. As depicted by Fig. 2a, dynamic sea level rise at the midlatitudes, especially in the Pacific and Indian Oceans causes higher probabilities of exceedance of hazard thresholds at these locations. The impacts of glacier mass balance change on sea level, as depicted in Fig. 2c, create relatively low probabilities of exceedance at northern latitudes, especially near Greenland and for lower threshold values. Sea level rise exceedance probabilities are low across all thresholds at the most southern latitudes, reflecting patterns of Antarctic mass loss and dynamic sea level rise, as depicted in Figs. 2a and 2e respectively.

b. *Deaggregation of forcing scenarios and sea level rise predictions*

Probabilistic sea level rise hazard analysis allows for the deaggregation of sea level rise hazard into its contributing sources, models, and scenarios. Deaggregations in this study are found using global mean sea level rise, calculated using the relative surface areas of different grid cells. As depicted in Fig. 4, the contributions of different RCPs vary with respect to sea level rise threshold. At thresholds less than 50 cm, conditional probabilities for each RCP are similar. This occurs because all scenarios project at least this much global mean sea level rise by 2100. At higher sea level rise thresholds, the conditional

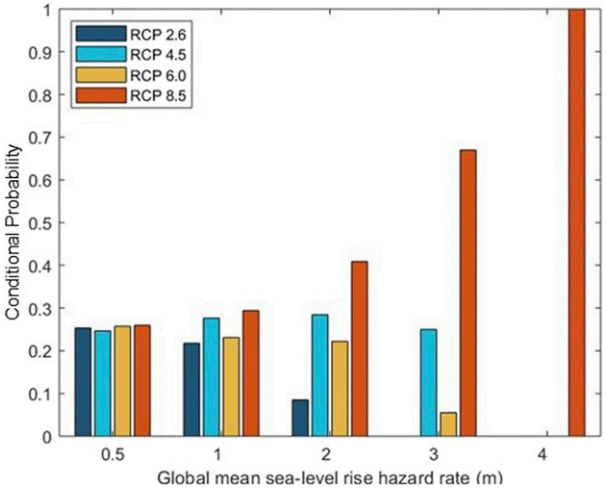

FIG. 4. Probabilities of RCP forcing scenarios given exceedance of 2006–2100 global mean sea level rise hazard thresholds.

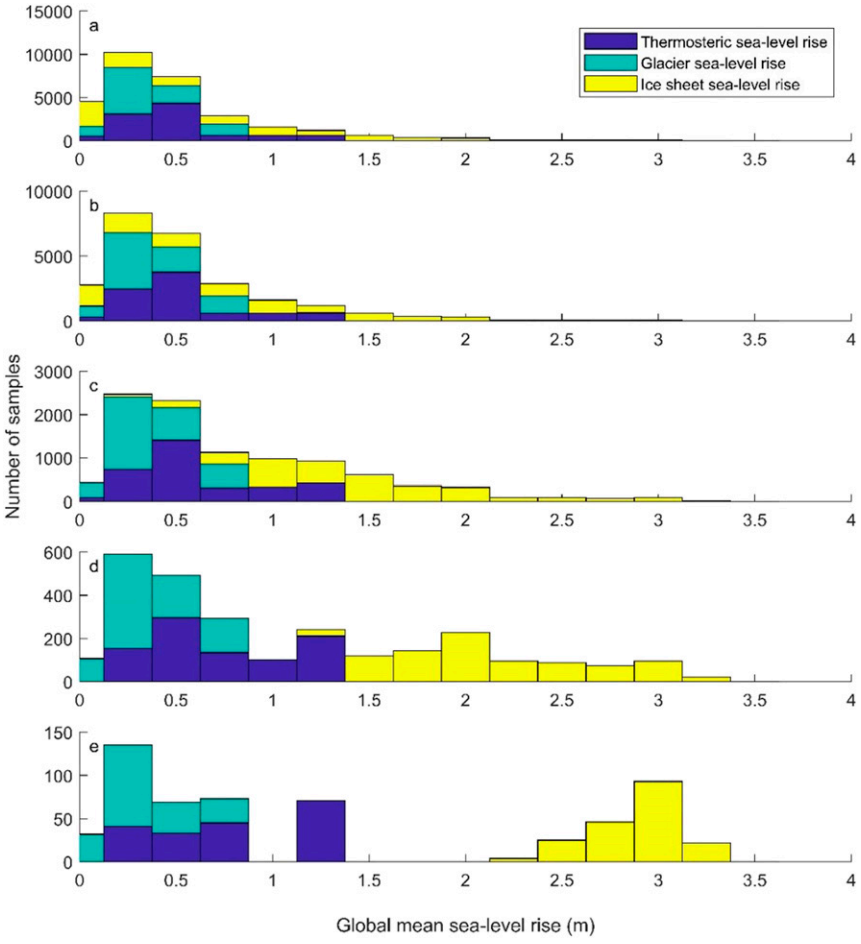

FIG. 5. Histograms of the magnitudes of 2006–2100 global mean thermosteric, glacier, and ice sheet sea level rise given exceedance of (a) 0.5, (b) 1, (c) 2, (d) 3, and (e) 4 m hazard thresholds.

probabilities of RCP2.6, RCP6.0, and RCP4.5 drop, reflecting the relatively low sea level rise predicted by these scenarios. It is not very surprising that projections of RCP4.5 are larger than those for RCP6.0, as RCP4.5 projects higher growth in radiative forcing early in the twenty-first century than RCP6.0. In probabilistic sea level rise hazard analysis, there is no point where mitigation scenarios such as RCP2.6 will contribute more to higher sea level rise thresholds than more extreme scenarios.

In this illustrative study, the probabilities that sea level rise exceeds a given threshold are deaggregated both categorically, among RCPs and sea level rise prediction models, and for the magnitude of predicted sea level rise. Such analyses can help us consider the importance of different contributions. Figure 5 depicts conditional histograms of global mean thermosteric, glacier, and ice sheet sea level rise. Samples of thermosteric sea level rise vary significantly in magnitude, ranging from as low as 0.25 m to as high as 1.25 m between 2006 and 2100. As hazard thresholds increase, fewer and fewer predictions exceed the threshold and the lowest sea level rise predictions stop contributing to the exceedance rate. Interestingly, thresholds have minimal impact on the global mean glacier contribution. Although glacier contributions range from 0.20 to 0.85 m and are of similar magnitude to other sources of sea level rise, they are not found to be strongly correlated with overall sea level rise for any given sample. The ice sheet contribution has a strong correlation with total sea level rise. Due to a relatively wide prediction range among ISMs, the ice sheet contribution to sea level rise ranges from near 0 m to as high as 3.4 m, which is consistent with the range of possible ice sheet projections found in the literature (Wong et al. 2017). The highest overall sea level rise predictions result from especially large ice sheet contributions. Uncertainty with respect to the ice sheet sea level rise contribution likely coincides with different modeling assumptions about ice sheet instability (DeConto and Pollard 2016; Ruckert et al. 2017).

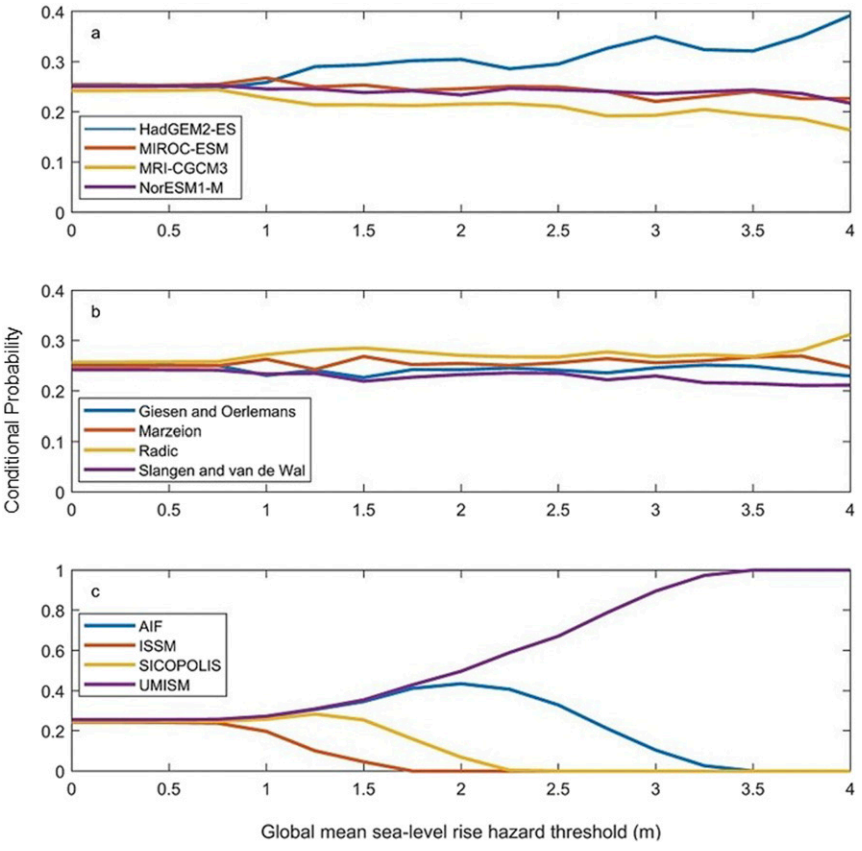

FIG. 6. Probabilities of (a) GCMs, (b) glacier models, and (c) ice sheet models given exceedance of 2006–2100 global mean sea level rise hazard thresholds.

Figure 6 depicts the relative contributions of GCMs, glacier models and ISMs. As hazard thresholds increase, the HadGEM2-ES model grows in importance, reflecting the fact that other GCMs more rarely predict sufficient thermosteric sea level rise to create overall mean sea level change as large as 4 m. Glacier model contributions are not strongly affected by hazard threshold, with model contributions only increasing or decreasing very slightly with increases in threshold. The contributions of ISMs have a strong connection to hazard rate, with UMISM dominating the most extreme ice sheet sea level rise contributions. In comparison, the ISSM contribution fails to contribute at hazard thresholds greater than 1 m. The ice sheet contribution to sea level rise is the most significant source of uncertainty in understanding future sea level rise at this time.

5. Summary and discussion

In this study, we use probabilistic hazard analysis methods to model total sea level rise. A probabilistic distribution of total sea level rise is estimated using a set of forcing scenarios and a sea level rise prediction model sampling process, where simulations of thermosteric sea level rise, glacier melt, and ice sheet mass balance using different models are considered. This process facilitates aggregation of sources of sea level rise, allowing for the creation of sea level rise hazard maps that estimate the probability of exceeding a given sea level rise across the globe. Hazard maps demonstrate how the fingerprints of different sources of sea level rise combine to create distinct patterns of sea level rise and sea level rise uncertainty.

Hazard deaggregation allows us to consider the relative importance of different sources of sea level rise. Deaggregation among forcing scenarios reinforces the fact that climate forcing has a strong influence on sea level rise exceeding a given threshold. Understanding sea level rise at high hazard thresholds depends on understanding the response to extreme climate forcing. Among the physical processes driving sea level rise, the glacier contribution was found to have minimal impact on exceedance probabilities while the ice sheet contribution was found to have the greatest impact. The relative novelty of ISMs leads to a wide range of ice

sheet sea level rise projections, affecting overall sea level rise uncertainty. Thermosteric and dynamic sea level rise have a more moderate impact on sea level rise projections.

The probabilistic hazard analysis framework provides a pathway toward creating useful tools for decision-makers like hazard maps that give a single metric for total sea level rise projection uncertainty at specific hazard thresholds. Through hazard deaggregation, this study illustrates how this framework could be implemented and highlights how sea level rise projection uncertainty is sensitive to climate forcing scenarios and sea level rise contribution projections. If official hazard analysis products are to be created in the future, decision-makers should aim to create more comprehensive forcing scenario and sea level rise prediction ensembles and will need to confirm specifics of the overall probabilistic sea level rise model.

Acknowledgments. We acknowledge the World Climate Research Programme's Working Group on Coupled Modeling, which is responsible for CMIP, and we thank the institutes for the climate models for producing and making available their model output. The U.S. Department of Energy's Program for Climate Model Diagnosis and Intercomparison provides coordinating support and led development of software infrastructure in partnership with the Global Organization for Earth System Science Portals for CMIP5. We acknowledge the Intergovernmental Panel on Climate Change Fifth Assessment Report, which included an emulation strategy for estimating glacier contributions to sea level rise for four glacier models. We acknowledge the Jet Propulsion Laboratory's GRACE measurement of monthly mass grids available at http://grace.jpl.nasa.gov, supported by the NASA MEaSUREs Program. We acknowledge the community organized SeaRISE project, which makes available data about ice sheet basin atmospheric and ocean response parameters. We acknowledge the Commonwealth Scientific and Industrial Research Organization (CSIRO) for combining and making available TOPEX/Poseidon, *Jason-1*, *Jason-2*/OSTM, and *Jason-3* satellite altimetry measurements of sea level, available at https://www.cmar.csiro.au/sealevel/sl_data_cmar.html. This work was supported in part by the Committee on Research at Marquette University, under the Regular Research Grant and the Summer Faculty Fellowship awarded to the Principal Investigator T.L., the second author. The Regular Research Grant provides research assistantship support for the first author M.A.T., along with the Research Leaders Fellowship from the Opus College of Engineering. In addition, the capital and operating support from the Office of the Provost to T.L.'s Multi-Hazard Sustainability (HazSus) Research Group is gratefully acknowledged.

REFERENCES

Adhikari, S., E. R. Ivins, and E. Larour, 2016: ISSM-SESAW v1.0: Mesh-based computation of gravitationally consistent sea-level and geodetic signatures caused by cryosphere and climate driven mass change. *Geosci. Model Dev.*, **9**, 1087–1109, https://doi.org/10.5194/gmd-9-1087-2016.

Cornell, C. A., 1968: Engineering seismic risk analysis. *Bull. Seismol. Soc. Amer.*, **58**, 1583–1606.

DeConto, R. M., and D. Pollard, 2016: Contribution of Antarctica to past and future sea-level rise. *Nature*, **531**, 591–597, https://doi.org/10.1038/nature17145.

Ebi, K. L., and Coauthors, 2013: A new scenario framework for climate change research: Background, process, and future directions. *Climatic Change*, **122**, 363–372, https://doi.org/10.1007/s10584-013-0912-3.

Fyke, J. G., A. J. Weaver, D. Pollard, M. Eby, L. Carter, and A. Mackintosh, 2011: A new coupled ice sheet/climate model: Description and sensitivity to model physics under Eemian, Last Glacial Maximum, late Holocene and modern climate conditions. *Geosci. Model Dev.*, **4**, 117–136, https://doi.org/10.5194/gmd-4-117-2011.

Giesen, R. H., and J. Oerlemans, 2012: Calibration of a surface mass balance model for global-scale applications. *Cryosphere*, **6**, 1463–1481, https://doi.org/10.5194/tc-6-1463-2012.

IPCC, 2013: *Climate Change 2013: The Physical Science Basis*. Cambridge University Press, 1535 pp., https://doi.org/10.1017/CBO9781107415324.

Landerer, F. W., P. J. Gleckler, and T. Lee, 2013: Evaluation of CMIP5 dynamic sea surface height multi-model simulations against satellite observations. *Climate Dyn.*, **43**, 1271–1283, https://doi.org/10.1007/s00382-013-1939-x.

Levermann, A., and Coauthors, 2014: Projecting Antarctic ice discharge using response functions from SeaRISE ice-sheet models. *Earth Syst. Dyn.*, **5**, 271–293, https://doi.org/10.5194/esd-5-271-2014.

Lin, T., 2012: Probabilistic sea-level rise hazard analysis. *Sustainable Civil Infrastructures—Hazards, Risk, Uncertainty*, K. K. Phoon et al., Eds., Research Publishing Services, 593–598, https://doi.org/10.3850/978-981-07-2219-7_P296.

——, and J. W. Baker, 2011: Probabilistic seismic hazard deaggregation of ground motion prediction models. *Fifth Int. Conf. on Earthquake Geotechnical Engineering*, Santiago, Chile, International Society for Soil Mechanics and Geotechnical Engineering, 12 pp.

——, S. C. Harmsen, J. W. Baker, and N. Luco, 2013: Conditional spectrum computation incorporating multiple causal earthquakes and ground motion prediction models. *Bull. Seismol. Soc. Amer.*, **103**, 1103–1116, https://doi.org/10.1785/0120110293.

Marzeion, B., A. H. Jarosch, and M. Hofer, 2012: Past and future sea-level change from the surface mass balance of glaciers. *Cryosphere*, **6**, 1295–1322, https://doi.org/10.5194/tc-6-1295-2012.

Mengel, M., A. Levermann, K. Frieler, A. Robinson, B. Marzeion, and R. Winkelmann, 2016: Future sea level rise constrained by observations and long-term commitment. *Proc. Natl. Acad. Sci. USA*, **113**, 2597–2602, https://doi.org/10.1073/pnas.1500515113.

Moss, R. H., and Coauthors, 2010: The next generation of scenarios for climate change research and assessment. *Nature*, **463**, 747–756, https://doi.org/10.1038/nature08823.

Nakicenovic, N., and Coauthors, 2000: Special report on emissions scenarios. Cambridge University Press, 595 pp., https://www.ipcc.ch/site/assets/uploads/2018/03/emissions_scenarios-1.pdf.

Nauels, A., J. Rogelj, C.-F. Schleussner, M. Meinshausen, and M. Mengel, 2017: Linking sea level rise and socioeconomic indicators under the Shared Socioeconomic Pathways. *Environ. Res. Lett.*, **12**, 114002, https://doi.org/10.1088/1748-9326/aa92b6.

Nowicki, S., and Coauthors, 2013a: Insights into spatial sensitivities of ice mass response to environmental change from the SeaRISE ice sheet modeling project I: Antarctica. *J. Geophys. Res. Earth Surf.*, **118**, 1002–1024, https://doi.org/10.1002/jgrf.20081.

——, and Coauthors, 2013b: Insights into spatial sensitivities of ice mass response to environmental change from the SeaRISE ice sheet modeling project II: Greenland. *J. Geophys. Res. Earth Surf.*, **118**, 1025–1044, https://doi.org/10.1002/jgrf.20076.

Peltier, W. R., 2004: Global glacial isostasy and the surface of the ice-age Earth: The ICE-5G (VM2) Model and GRACE. *Annu. Rev. Earth Planet. Sci.*, **32**, 111–149, https://doi.org/10.1146/annurev.earth.32.082503.144359.

Radić, V., A. Bliss, A. C. Beedlow, R. Hock, E. Miles, and J. G. Cogley, 2013: Regional and global projections of twenty-first century glacier mass changes in response to climate scenarios from global climate models. *Climate Dyn.*, **42**, 37–58, https://doi.org/10.1007/s00382-013-1719-7.

Ruckert, K. L., G. Shaffer, D. Pollard, Y. Guan, T. E. Wong, C. E. Forest, and K. Keller, 2017: Assessing the impact of retreat mechanisms in a simple Antarctic ice sheet model using Bayesian calibration. *PLOS ONE*, **120**, e0170052, https://doi.org/10.1371/journal.pone.0170052.

Slangen, A. B. A., and R. S. W. van de Wal, 2011: An assessment of uncertainties in using volume-area modelling for computing the twenty-first century glacier contribution to sea-level change. *Cryosphere*, **5**, 673–686, https://doi.org/10.5194/tc-5-673-2011.

Swenson, S. C., 2012: GRACE monthly land water mass grids NETCDF release 5.0. Ver. 5.0. PO.DAAC, accessed 15 February 2018, https://doi.org/10.5067/TELND-NC005.

Taylor, K. E., R. J. Stouffer, and G. A. Meehl, 2012: An overview of CMIP5 and the experiment design. *Bull. Amer. Meteor. Soc.*, **93**, 485–498, https://doi.org/10.1175/BAMS-D-11-00094.1.

Van Vuuren, D. P., and T. R. Carter, 2013: Climate and socioeconomic scenarios for climate change research and assessment: Reconciling the new with the old. *Climatic Change*, **122**, 415–429, https://doi.org/10.1007/s10584-013-0974-2.

Vizcaino, M., U. Mikolajewicz, F. Ziemen, C. B. Rodehacke, R. Greve, and M. R. van den Broeke, 2015: Coupled simulations of Greenland Ice Sheet and climate change up to A.D. 2300. *Geophys. Res. Lett.*, **42**, 3927–3935, https://doi.org/10.1002/2014GL061142.

Winkelmann, R., A. Levermann, K. Frieler, and M. A. Martin, 2012: Uncertainty in future solid ice discharge from Antarctica. *Cryosphere Discuss.*, **6**, 673–714, https://doi.org/10.5194/tcd-6-673-2012.

Wong, T. E., A. M. R. Bakker, and K. Keller, 2017: Impacts of Antarctic fast dynamics on sea-level projections and coastal flood defense. *Climatic Change*, **144**, 347–364, https://doi.org/10.1007/s10584-017-2039-4.